Conversion of methane and carbon dioxide into synthesis gas over alumina-supported nickel catalysts. Effect of Ni–Al_2O_3 interactions

Yang-guang Chen and Jie Ren

Institute of Coal Chemistry, Chinese Academy of Sciences, PO Box 165, Taiyuan, Shanxi 030001, PR China

Received 11 November 1993; accepted 15 June 1994

A series of alumina-supported nickel catalysts were prepared by calcination of the catalyst precursors in air at different temperatures. The increase in the intensity of Ni–Al_2O_3 interactions with the calcination temperature was found to be unfavourable to the reduction of the catalyst, and thus caused a decrease in activity for the low temperature reaction between methane and carbon dioxide. However, the catalyst with strong Ni–Al_2O_3 interactions suppressed carbon deposition effectively, which can be attributed to the formation of spinel, $NiAl_2O_4$, after calcination. When the reaction was carried out at 1023 K, all the catalysts tended to exhibit the same activity. At the same time, only filamentous carbon with a hollow inner channel was observed and there were nickel particles on the tip of this filamentous carbon.

Keywords: conversion of methane; synthesis gas; alumina-supported nickel catalyst; metal–support interactions; carbon dioxide reforming

1. Introduction

Steam reforming and partial oxidation are two established industrial processes for converting methane to synthesis gas rich in hydrogen, which acts as a feedstock for the synthesis of ammonia and methanol. But recently, there is a growing interest in the production of synthesis gas by reforming methane with carbon dioxide, a cheap carbon-containing material. Since thus obtained gas product consists of equal amounts of hydrogen and carbon monoxide, it is particularly suitable to produce higher hydrocarbons and oxygenated derivatives. Meanwhile, as a hopeful new route to the rational use of carbon dioxide, this process is of great significance in environmental protection.

Only a few papers have been published concerning the reaction between methane and carbon dioxide, and most of them focus on the examination of catalytic activity and stability [1–5]. So little is available to understand the mechanism of this reaction, as well as the decisive cause for catalyst deactivation. Gadalla and

Sommer [1] have studied the effect of support, suggesting that supported nickel catalysts may lose their activity due to carbon deposition, the increase of Ni particle size and phase transformation such as the formation of $NiAl_2O_4$ spinel. They used thermodynamic calculations to establish the conditions for carbon deposition. However, the reaction in their studies was carried out at high temperatures (usually above 1200 K), where carbon deposition is thermodynamically avoidable. However, to use the catalysts industrially, a lower reaction temperature is desirable, so a different catalytic behaviour is expected.

It is well known that deactivation of supported Ni catalysts by carbon deposition is a problem of serious magnitude in steam reforming. It shows twofold: (1) fouling of the nickel surface, (2) blockage of the pore mouths which can also produce physical disintegration of the catalyst support [6]. But how does carbon deposition influence the stability of catalyst during the reforming of methane with carbon dioxide? What are the morphological properties of deposited carbon in this process? How do metal–support interactions affect the amount of deposited carbon? All these questions are not clear yet.

This paper reports the influence of Ni–Al_2O_3 interactions on the catalytic properties of Ni/Al_2O_3 during CO_2 reforming, by which we can obtain some information helpful to the understanding of the above questions.

2. Experimental

The catalysts were prepared by using the impregnation method. The support γ-Al_2O_3 (20–40 mesh) has a BET area of 160 m^2/g, and a pore volume of 1.28 ml/g. The nickel content was 13 wt%. The catalysts were calcined in air respectively at 573, 773, 973 and 1023 K for 2 h. The activity investigations were conducted in a flow reactor (an 8 mm i.d. quartz tube). 1 or 0.36 g catalysts were used. Before reaction, the catalysts were reduced with H_2 at 293 K for 4 h. Afterwards, H_2 was replaced by Ar and the temperature was adjusted to its desired value, and then the feed gas ($CO_2/CH_4 = 1:2$) was introduced, at 3000 h^{-1}/8700 h^{-1} space velocity under atmospheric pressure. The reactor inlet and outlet gas compositions were analysed by an on-line gas chromatograph (GC) equipped with a separating column of activated carbon.

The procedures of temperature-programmed reduction (TPR) and temperature-programmed desorption (TPD) used in this study were similar to those described in the literature [6]. TPR conditions were as follows: amount of catalyst, 0.2 g; gas mixture, 8.61% H_2/Ar; flow rate, 40 ml/min; heating rate, 15 K/min; temperature range, room temperature to 1153 K. In the TPD experiment, after reduction in H_2 at 923 K, 0.2 g of the catalyst was flushed with Ar and cooled to 573 K. Consequently, the pure CO_2 was adsorbed to saturation coverage. After the excess gas was removed by Ar, the catalyst was programmed heated to 1153 K at 20 K/min. A carrier gas of Ar at atmospheric pressure flowed through the catalyst at 40 ml/min. In the two cases, the signal from the thermal conductivity cell was continuously recorded.

X-ray photoelectron spectroscopy measurements were performed in a PHI 5300 ESCA spectrometer using Mg Kα radiation. The binding energies (BE) were calibrated against the C 1s 284.6 eV line. For the reduced samples, the transfer to the analytical chamber was under the protection of N_2.

Phase analysis of the catalysts was carried out in a D/max-γA X-ray diffractometer using Cu Kα radiation. The morphology of the catalysts was observed by means of a H-600-2 electron microscope.

3. Results and discussion

The influence of calcination temperature on conversions of methane and carbon dioxide is shown in fig. 1. At the low reaction temperature of 873 K, the following activity sequence was established: C573 > C773 > C973. Obviously, the activity decreased with increasing calcination temperature. But at the high reaction temperature of 1073 K, the differences in activity among these catalysts became rather smaller.

The stability of catalytic activity was examined at 1023 K for the three catalysts. A high space velocity of 8700 h^{-1} was used. It was seen that the conversion and product distribution remained constant during the reaction. Table 1 shows the data taken from the reaction running for 3 h. The amounts of deposited carbon demonstrated an intense carbon deposition on C573, whereas relatively less carbon formation occurred on C1023. A trend should readily be noted that the increase of calcination temperature was of great advantage to the suppression of carbon

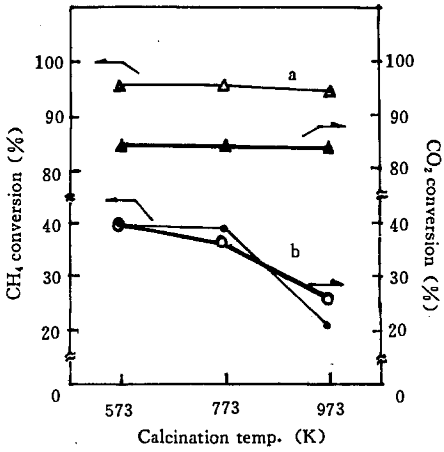

Fig. 1. Methane and carbon dioxide conversions versus calcination temperature. CO_2/CH_4: 1 : 2; pressure: atmospheric pressure; space velocity: 3000 h^{-1}. (a) Reaction temperature: 1073 K, (b) reaction temperature: 873 K.

Table 1
Activity and the amount of deposited carbon [a]

Catalyst	H_2 and CO in effluent gas (%)		Amount of deposited carbon (g/g-cat)
	H_2	CO	
C573	36.33	43.46	78.67
C773	35.76	42.82	50.91
C973	34.47	43.12	2.82
C1023	34.43	42.69	0.76

[a] Reaction temperature: 1023 K; space velocity: 8700 h^{-1}; CO_2/CH_4 ratio: 1 : 2; reaction time: 3 h.

deposition. Based on this result, we chose C1023 to examine its stability, and found that it was the most effective as regards the resistance to carbon deposition. The amount of carbon was reduced by a factor of 1% of that on C573.

TPR and TPD are two useful techniques for characterization of interactions between metal and support. TPR patterns (see fig. 2) presented the following order of maximum peak temperature: C973 > C923 > C873 > C673 > C573. This indicates that the Ni–Al_2O_3 interactions are affected by the calcination temperature. The higher the calcination temperature, the stronger the Ni–Al_2O_3 interaction.

Fig. 3 shows CO_2 TPD patterns of the catalysts and the blank support γ-Al_2O_3. It reveals that the loading of Ni results in the formation of a low-temperature peak starting from 577 K, although the area of this part is relatively smaller than that desorbing at least from above 773 K in a broad peak expanding over the temperature range studied here. The latter peak is the common characteristic of both the catalysts and blank support. No CO was detected desorbing from the catalyst

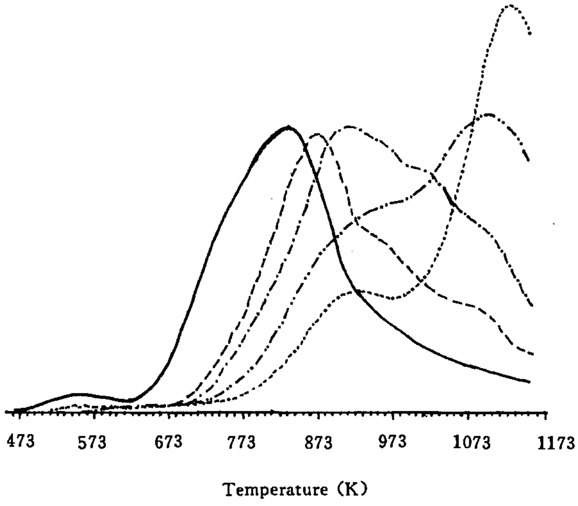

Fig. 2. TPR patterns of C573, C673, C873, C923, C973. (——) C573; (– – –) C673; (–·–) C873; (–··–) C923; (- - -) C973.

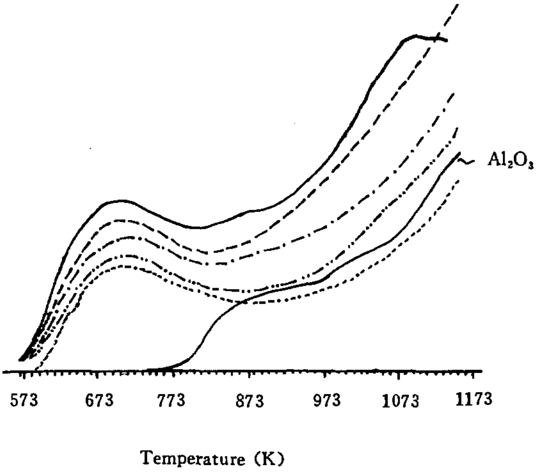

Fig. 3. CO_2 TPD patterns of C573, C673, C873, C973, C1023. (——) C573; (- - -) C673; (-·-) C873; (-··-) C973; (-·-·-) C1023.

following CO_2 adsorption. This observation agrees with that reported by Zagli et al. [7]. They believed that most desorbed CO_2 was originating from the CO_2 adsorbed on the γ-Al_2O_3 support. However, from our results the loading of Ni enhanced the capacity of CO_2 adsorption, only the increment decreased with increasing the calcination temperature. It is probably due to the diffusion of Ni from surface to bulk resulting from the strong Ni–Al_2O_3 interactions.

Fig. 4 shows the XRD patterns of some selected catalysts after calcination, reduction and reaction. Along with the increase of calcination temperature, the calcined catalysts exhibited decreasing intensities of broad lines at $2\theta = 37.4$–$37.7°$, 43.5–43.7° and 63.1–63.2° which correspond to NiO. At the same time, an increase in the intensities of broad lines at $2\theta = 37.4$–$37.7°$, 45.9–46° and 66.8–66.9° is also observed for C973 and C1023, indicating the appearance of $NiAl_2O_4$. The blue color of C973 and C1023 gives further support to this finding. Upon reduction, metallic nickel lines at $2\theta = 52$–$52.2°$ and 44.6–44.8° appeared accompanied by the disappearance of NiO, while $NiAl_2O_4$ lines are retained. After reaction, the only apparent variation in comparison with the reduced catalysts is the formation of the graphite line at $2\theta = 26.2°$ in C573 and C773. The graphite peak on C573 is larger than on C773, which is identical to the data of carbon deposition. These results reveal that the bulk of reduced C973 and C1023 is a mixture of metallic nickel and $NiAl_2O_4$, especially in C1023 a large quantity of $NiAl_2O_4$ is formed, whereas the other catalysts exhibited a predominant Ni^0 with NiO detectable only in the calcined forms. It seems that the low activity for low temperature reaction and the good resistance to carbon deposition of C1023 are related to the formation of $NiAl_2O_4$.

Being sensitive to the composition of the top surface layers, XPS measurements

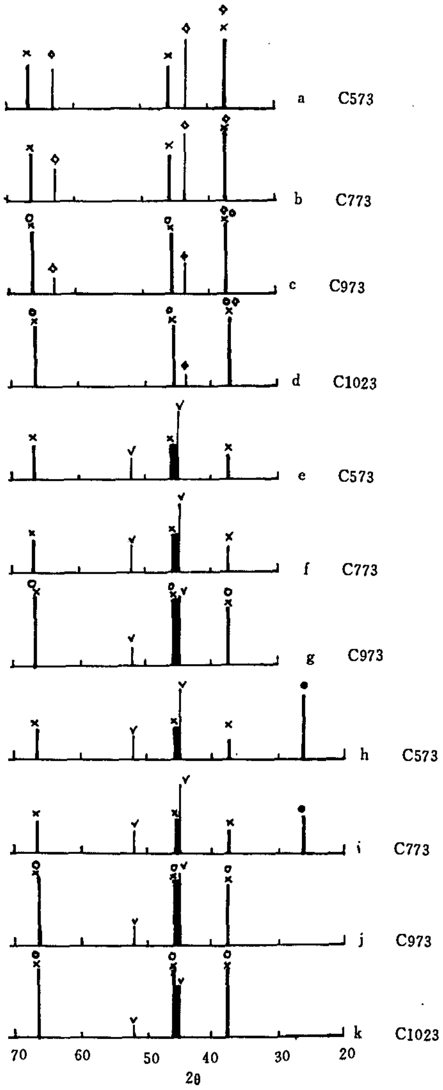

Fig. 4. XRD patterns of selected catalysts after calcination, reduction and reaction. (a–d) After calcination; (e–g) after reduction; (h–k) after reaction. (×) Al_2O_3; (◇) NiO; (✓) Ni^0; (○) $NiAl_2O_4$; (●) C graphite.

are employed in determining the state of surface nickel in the catalysts. The calcined catalysts C573 and C1023 gave a broad peak with the BE maximum of the Ni $2p_{3/2}$ transition centered at 855.5 and 855.8 eV respectively (fig. 5). For reduced catalysts, Ni^0 was found in C573, C673 and C873 with Ni $2p_{3/2}$ BE between 851.7 and 852.4 eV, but did not exist in C973 and C1023, indicating that the latter two catalysts are too difficult to be reduced. This result is consistent with those from TPR. It is worthy of note that an increase in the BE of Ni $2p_{3/2}$ from 855.2 to 855.9 eV, which can be identified as Ni^{2+}, is observed parallel to the increase of cal-

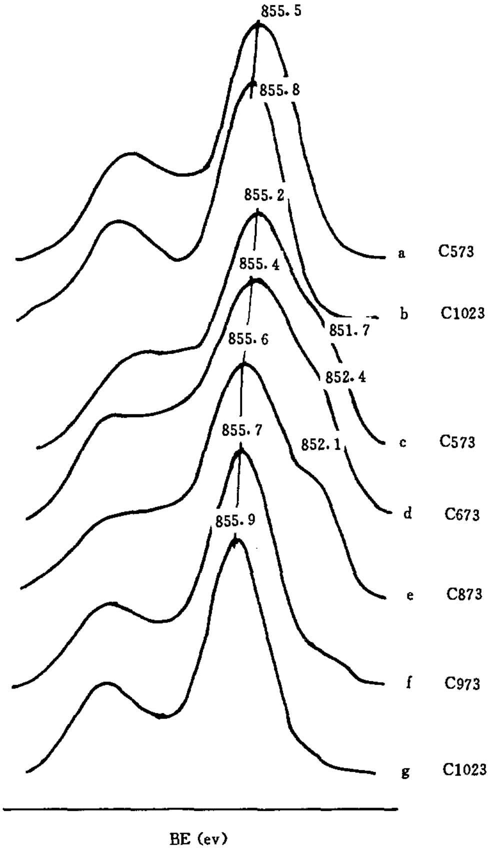

Fig. 5. XPS patterns of selected catalysts after calcination and reduction. (a–b) After calcination; (c–g) after reduction.

cination temperature, suggesting a progressive transformation from NiO to spinel. For reduced C573 and C773, XRD measurements indicate the existence of significant metallic nickel but not NiO, while XPS results suggest that the surface species are composed of Ni^0 and Ni^{2+}. This disagreement may be associated with the surface partial oxidation of the catalysts during the preparation of XPS samples following reaction. C973 and C1023 showed a similar possibility.

Since the reduced C1023 behaves distinctly from the reduced C573 in the surface chemical states of nickel, why does C1023 exhibit about the same activity as C573 at reaction temperature of 1023 K (see table 2). In order to explain this phenomenon, the activity of the calcined C1023 versus time-on-stream was investigated (table 2). As expected, the initial activity of the calcined C1023 was negligible. But when the reaction time was prolonged, the fraction of H_2 was first increased, which was coming from the gas decomposition of CH_4. The catalyst was then activated in the presence of H_2, and therefore became more and more active for the reaction.

Table 2
Activity for the calcined C1023 versus time-on-stream [a]

	Reaction time (h)			
	0.0	0.5	1.0	1.5
CO (%)	0.14	0.11	42.16	42.61
H_2 (%)	0.0	17.26	29.63	34.44
CO + H_2 (%)	0.14	17.37	71.79	77.05

[a] Reaction temperature: 1023 K; CO_2/CH_4: 1 : 3; space velocity: 3000 h^{-1}.

After 1.5 h, the reaction reached a steady state, where the yield of H_2 + CO leveled out at 77.05%. This reflects two facts as follows:

(1) the calcined spinel is not active,

(2) not only Ni^0 but also the reduced spinel makes a contribution towards activity.

Al-Ubaid and Wolf [8] have studied steam reforming of methane on reduced nonstoichiometric nickel aluminate catalysts prepared by co-precipitation. They pointed out that the calcined spinels are not active, but the reduced forms lead to significant activity and stability. It is speculated that the active nickel is present in a monodispersed form in special sites provided by the nickel aluminate structure, and not detected by XRD and XPS measurements. These can best account for our results.

We have evaluated a lot of catalysts. All of them do not lose their activity with time-on-stream. The longest run was carried out over 120 h, which will be reported in the near future. The drastic increase in the pressure drop sometimes forces the reaction to be interrupt. This is due to physical breakdown of the catalyst support resulting from carbon deposition, not phase transformation, proposed by Gadalla and Sommer [2]. This can be illustrated from the amount of deposited carbon and XRD phase analysis (fig. 4). Electron micrographs of all catalysts after reaction show that only filamentous carbon was observed in the form of a Ni particle on the tip of filamentous carbon with a hollow inner channel (fig. 6). According to our results of CO disproportionation, the disproportionation does not occur above 973 K in the presence of the catalysts, which agrees with the thermodynamic calculations (table 3) [9].

We can draw the conclusion that carbon deposition in CO_2 reforming is mainly produced by the catalytic decomposition of CH_4. Thereby the possible mechanism for the formation of carbon from the decomposition of CH_4 on metal surfaces is also applicable to CO_2 reforming. As seen in fig. 6, a large amount of filamentous carbon was formed on C573 rather than on C1023. This indicates that a superior structure provided by the reduced spinel can resist the segregation of Ni from spinel, and therefore reduce the formation of carbon.

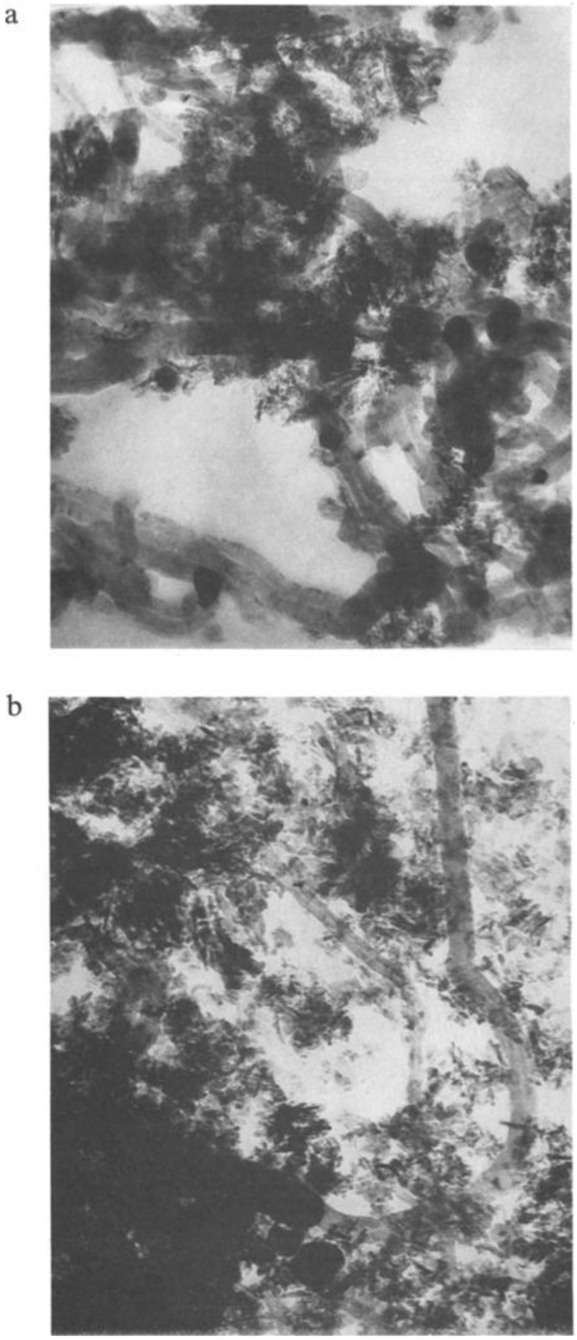

Fig. 6. TEM photomicrographs for C573 and C1023 after reaction (100 × 1000). (a) C573; (b) C1023.

Table 3
Equilibrium constant for carbon deposition reaction [a]

Reaction	K_P
$CH_4 \rightleftharpoons C + 2H_2$	13.182
$2CO \rightleftharpoons C + CO_2$	0.347
$CO + H_2O \rightleftharpoons C + H_2O$	0.279

[a] Reaction pressure: atmospheric pressure; reaction temperature: 1023 K.

4. Conclusion

(1) The formation of surface spinel, $NiAl_2O_4$, has a good effect on the suppression of carbon deposition, and it exhibits a high activity at high reaction temperatures (at or above 1023 K).

(2) Only filamentous carbon with a nickel crystal at the top was observed at the reaction temperature of 1023 K. The decomposition of CH_4 is suggested to be the main reaction to form carbon.

(3) Phase transformation does not occur under our reaction conditions. The carbon deposition is responsible for the increased pressure drop.

References

[1] A.M. Gadalla and B. Bower, Chem. Eng. Sci. 43 (1988) 3049.
[2] A.M. Gadalla and M.E. Sommer, Chem. Eng. Sci. 44 (1989) 2825.
[3] J.S.H.Q. Perera, J.W. Couves, G. Sanker and J.M. Thomas, Catal. Lett. 11 (1991) 219.
[4] F. Solymosi, Gy. Kutsan and A. Erdohelyi, Catal. Lett. 11 (1991) 149.
[5] T. Sodesawa, A. Dobashi and F. Nozaki, React. Kinet. Catal. Lett. 12 (1979) 107.
[6] C.H. Bartholomew, Catal. Rev.-Sci. Eng. 24 (1982) 67.
[7] A.E. Zagli, J.L. Falconer and C.A. Keenan, J. Catal. 56 (1979) 453.
[8] A. Al-Ubaid and E.E. Wolf, Appl. Catal. 40 (1988) 73.
[9] Shun Xixian et al., Chemical Journal of Chinese Universities 13 (1992) 1302.
[10] J.R. Rostrup-Nielsen, J. Catal. 48 (1977) 155.